

# Orange Fluorescent Ru(III) Complexes Based on 4'-Aryl Substituted 2,2':6',2''-Terpyridine for OLEDs Application

Raja Lakshmanan<sup>1</sup> · N. C. Shivaprakash<sup>2</sup> · S. Sindhu<sup>1</sup>

Received: 14 August 2017 / Accepted: 19 September 2017  
© Springer Science+Business Media, LLC 2017

**Abstract** A series of ruthenium (III) complexes of the formulae [Ru(4-Mephtpy)<sub>2</sub>]Cl<sub>3</sub>(1) [**Ru(L<sub>1</sub>)**], [Ru(3,4,5-tmphtpy)<sub>2</sub>]Cl<sub>3</sub>(2) [**Ru(L<sub>2</sub>)**], and [Ru(4-thtpy)<sub>2</sub>]Cl<sub>3</sub>(3) [**Ru(L<sub>3</sub>)**], (where L = terpy = 2,2':6',2'' terpyridine ligands) are synthesized. The complexes were characterized by elemental analyses, spectroscopic and electrochemical data. The density functional theory (DFT) outlines the geometric optimisation and electronic charge transition of these complexes. Photophysical studies describe that the luminescence of Ru(III) complexes is due to electronic transition between the energy levels of singly unoccupied molecular orbitals (SUMO) and singly occupied molecular orbitals (SOMO). It also exhibits the potential charge transfer to  $\pi-\pi^*$  and  $n-\pi^*$  states due to MLCT and ILCT processes of the complexes. The observed bands centered at 591 and 620 nm demonstrate that these emissions originated from the transition of SUMO to SOMO energy levels, that is, from the radiative decay from the doublet exciton. Due to the heavy metal effect of Ru(III) ions the photophysical behaviour depends on the MLCT process. In conclusion, that the all three **Ru(L<sub>1</sub>-L<sub>3</sub>)** complexes are fallen orange emission.

**Keywords** Photophysical properties · Ru(III) complexes · Orange fluorescent emitter · 2,2':6',2''-terpyridine · OLEDs

## Introduction

Recently, organometallic complexes are used widely to synthesize optoelectronic devices, such as organic solar cells and for OLEDs [1–5]. Transition metal-based organometallic complexes are of interest due to their versatile nature like ease of tuning the photophysical, electrochemical and magnetic properties [6–8]. These properties strongly depend on the oxidation states of the transition metal used in the complex. Among the various transition metals, ruthenium has gained interest in the preparation of organometallic complexes for OLED applications [9, 10]. Barthelmes et al. synthesised ruthenium-based terpy metal complexes and studied their photophysical and electrochemical properties [11]. Other research groups studied these and the thermal properties of Ru(II)-based pyridine complexes [12–14]. Many studies have been conducted on the synthesis and characterization of Ru(II)-based terpy complexes for luminescent applications [15, 16]. Kelch et al. studied the spectroscopic and electrochemical behaviour of rod-like ruthenium (II) coordination polymers [17] and observed deep orange emissions, strongly dependent on the nature of  $\pi$ -conjugated bis-terpy ligands. The spectroscopic and electrochemical properties of self-assembled metallo-polymers containing electron-donating and electron-withdrawing Ru(III)-based bis-terpy derivatives are still not clear [18, 19].

The luminescence and redox properties of Ru(III) complexes are of great interest among the researchers for their range of fundamental and practical applications [20, 21]. Ru(III)-based terpy complexes exhibit a strong orange emission with a suitable solvent. These emission bands could be due to the MLCT process of the complexes [22, 23]. The white light can be generated by mixing orange and blue emitters [24]. Heteroleptic ruthenium complexes have more advantages as functions of different groups can be integrated into

✉ S. Sindhu  
sindhunair@pilani.bits-pilani.ac.in

<sup>1</sup> Department of Physics, Birla Institute of Technology and Science, Pilani, Rajasthan 333031, India

<sup>2</sup> Department of Instrumentation and Applied Physics, Indian Institute of Science, Bangalore 560012, India

one molecule. Such complexes usually consist of two ligands with easily substituting functional groups. It has been observed that the functional groups in the ligand introduce interesting photophysical and electrochemical properties to the complexes [25, 26]. Researchers found that fluorine substitutions into the ligand can lower the HOMO energy level [27].

Phosphorescence is frequently detected in Ru(III) complexes at room temperature, which is attributed to the low-lying MLCT excited states. It has both ligand-centered (LC) and MLCT charge transition process [28, 29]. Extensive work has been carried out on dinuclear Ru(II) homo- and hetero-metallic complexes. In these complexes, the two metal centers are connected by an organic wire type bridge. The Ru(II)-based terpy complexes exhibit phosphorescence behaviour in a few microseconds, whereas Ru(III)-based terpy complexes exhibit similar characteristics in about a few nanoseconds [30, 31]. Hence, the photophysical and electrochemical behaviour of Ru ion depend on the oxidation states; it's interesting to study the oxidation states of Ru ion-based organometallic complexes [32, 33]. A lack of interest in the photochemical behaviour of Ru(III) derivatives arises from observations that although their lowest excited states are luminescent in glasses at low temperatures, they are essentially non-emissive and short-lived in solution at ambient temperature. It is necessary to introduce cyclo-metallated ligands to complexes for luminescence in solution [34].

In this work, the synthesis of a series of three new orange-fluorescent Ru(III)-based terpyridine complexes and their characteristics like photophysical, thermal and electrochemical for fluorescent OLED applications are discussed. The introduction of electron-donor substituents onto a terpy ligand results in fluorescent emission at room temperature in Ru(III) complexes. These are reflected in the electrochemical properties with the electron-releasing substituents stabilizing the Ru(III) state and lowering the potential of the Ru(II)/Ru(III) couples.

## Experimental

### Syntheses of Ru(III) Complexes (RuL<sub>1</sub>-L<sub>3</sub>)

The synthesis of terpyridine ligands, such as C<sub>1</sub> and C<sub>2</sub>, was published elsewhere [35]. Ligand C<sub>3</sub> was also synthesised using a procedure similar to that performed for ligands C<sub>1</sub> and C<sub>2</sub>. The following sections provide the details of preparation of metal complexes.

The complexes were prepared following a general synthetic route. An ethanolic solution (15 ml) of RuCl<sub>3</sub>·3H<sub>2</sub>O (0.26 g, 1.0 mmol) was added dropwise to a dichloromethane solution (15 ml) of the terpyridine ligand (4-Mephtpy,

0.32 g; 3,4,5-tmphtpy, 0.35 g; 1.0 mmol, 4-thtpty, 0.28 g; 1.0 mmol) with stirring. The reaction mixture was refluxed for 6 h to obtain a crystalline solid of the precursor complex, which was filtered, washed with ice-cold ethanol followed by diethyl ether and finally dried in a vacuum. Scheme 1 shows synthetic route of (RuL<sub>1</sub>-L<sub>3</sub>) complexes.

### [Ru(4-Mephtpy)<sub>2</sub>]Cl<sub>3</sub>: [Ru(L<sub>1</sub>)]

Yield: 67%, T<sub>m</sub>. 425 °C, Anal. Calcd for C<sub>44</sub>H<sub>34</sub>Cl<sub>3</sub>N<sub>6</sub>Ru: C, 61.87; H, 4.01; N, 9.84. Found: C, 61.69; H, 4.07; N, 9.87. IR (KBr):  $\nu$  = 3379 (w), 3308 (w), 3075 (w), 1586 (m), 1508 (m), 1461 (m), 1397 (m), 1306 (m), 1124 (w), 984 (s), 833 (m), 786 (m), 715 (s), 742 (w), 732 (s), 682 (m), 658 (m), 620 (m) cm<sup>-1</sup>. MS (ESI, *m/z*): 784.18 [M-3Cl]<sup>+</sup>.

### [Ru(3,4,5-tmphtpy)<sub>2</sub>]Cl<sub>3</sub>: [Ru(L<sub>2</sub>)]

Yield: 74%, T<sub>m</sub>. 429 °C, Anal. Calcd for C<sub>48</sub>H<sub>42</sub>Cl<sub>3</sub>N<sub>6</sub>O<sub>6</sub>Ru: C, 57.29; H, 4.21; N, 8.35. Found: C, 57.31; H, 4.23; N, 8.37. IR (KBr):  $\nu$  = 3379 (w), 3307 (w), 1586 (m), 1508 (m), 1397 (m), 1351 (m), 1308 (w), 1162 (s), 1124 (m), 884 (m), 833 (s), 786 (w), 715 (s), 647 (m) cm<sup>-1</sup>. MS (ESI, *m/z*): 899.94 [M-3Cl]<sup>+</sup>.

### [Ru(4-thtpty)<sub>2</sub>]Cl<sub>3</sub>: [Ru(L<sub>3</sub>)]

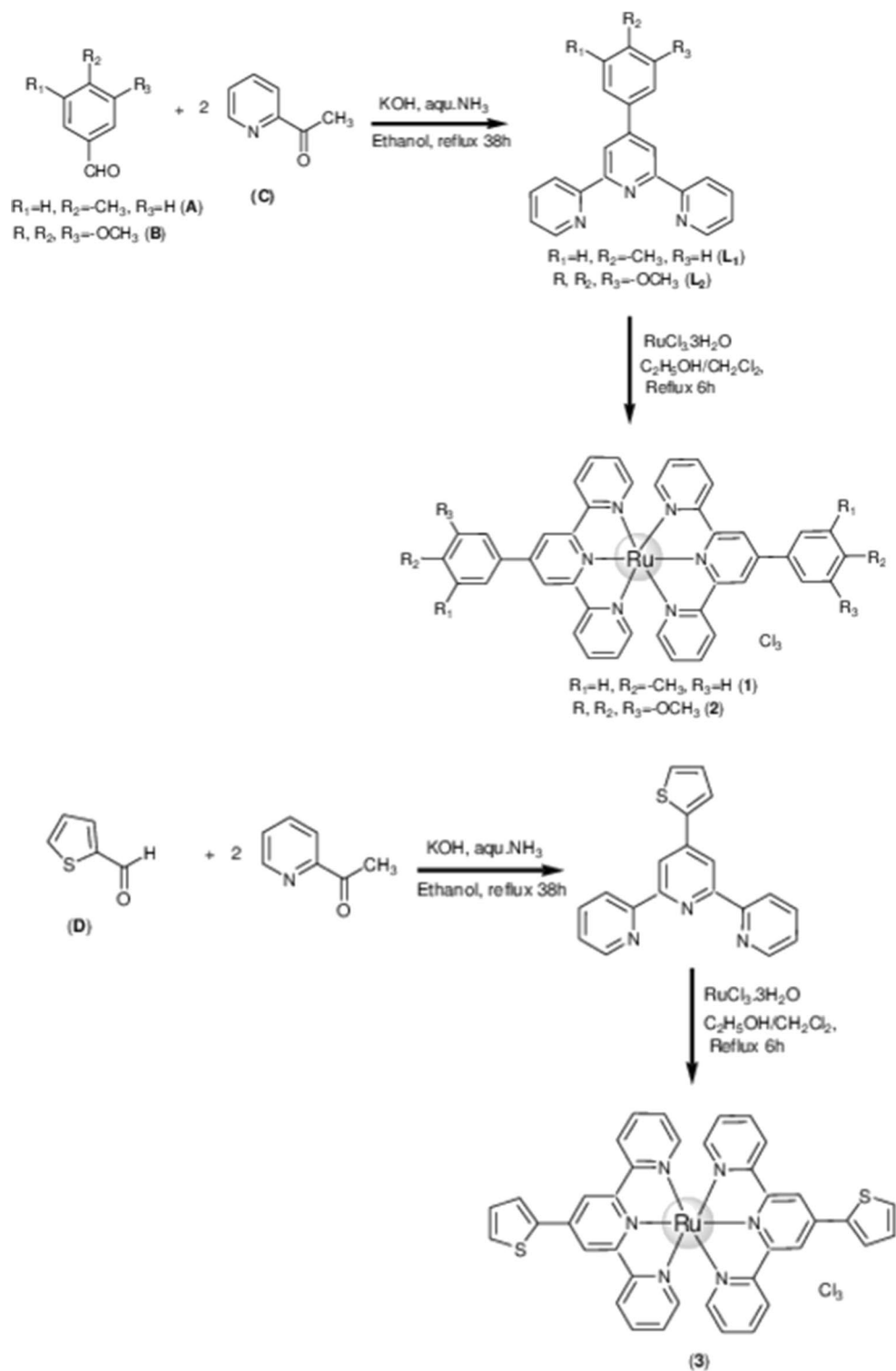
Yield: 68%, T<sub>m</sub>. 471 °C, Anal. Calcd for C<sub>38</sub>H<sub>26</sub>Cl<sub>3</sub>N<sub>6</sub>SRu: C, 56.62; H, 3.25; N, 10.42; S, 3.98. Found: C, 56.69; H, 3.28; N, 10.47; S, 3.97. IR (KBr):  $\nu$  = 3467 (w), 3056 (w), 3075 (w), 1595 (m), 1527 (m), 1414 (m), 1419 (m), 1359 (m), 1237 (w), 838 (s), 780 (s), 716 (s), 626 (m), 658 (m) cm<sup>-1</sup>. MS (ESI, *m/z*): 699.81 [M-3Cl]<sup>+</sup>.

## Quantum Calculation of Ru(L<sub>1</sub>-L<sub>3</sub>) Complexes

Geometric optimization and electronic structure of the Ru(L<sub>1</sub>-L<sub>3</sub>) complexes were achieved by DFT using a B3LYP/def2-TZvP basis set employing Gaussian-09 program [36]. In addition, energy levels of the frontier molecular orbitals (i.e., HOMO, SOMO, SUMO, and LUMO) of three Ru(III) complexes were also obtained. The FMOs along with individual contributions of Ru(III) complexes were fully optimized as shown in Fig. 1. FMOs have two types of charge transitions in the complexes MLCT and ILCT. MLCT can be attributed to charge transition between SOMO and SUMO energy levels of Ru ion. In ILCT, the charge transition takes place between SOMO/HOMO and the higher energy orbitals. This is mainly attributed to  $\pi$ - $\pi^*$  and  $n$ - $\pi^*$  of terpyridine ligands [37, 38].

In all the complexes, the SOMO energy level is mostly localized on the 4'-aryl substituent ring, whereas the SUMO energy is localized between Ru ion and the terpy

**Scheme 1** Synthetic route of Ru(III) terpyridine complexes (RuL1-L3)



ring. Therefore, the electronic emission processes of all complexes are mainly attributed to the Ru(III) ions, such as transition from SUMO to SOMO, that is, the radiative

decay takes place from the doublet excitons. The orange emission of the complexes is confirmed by PL spectra; the

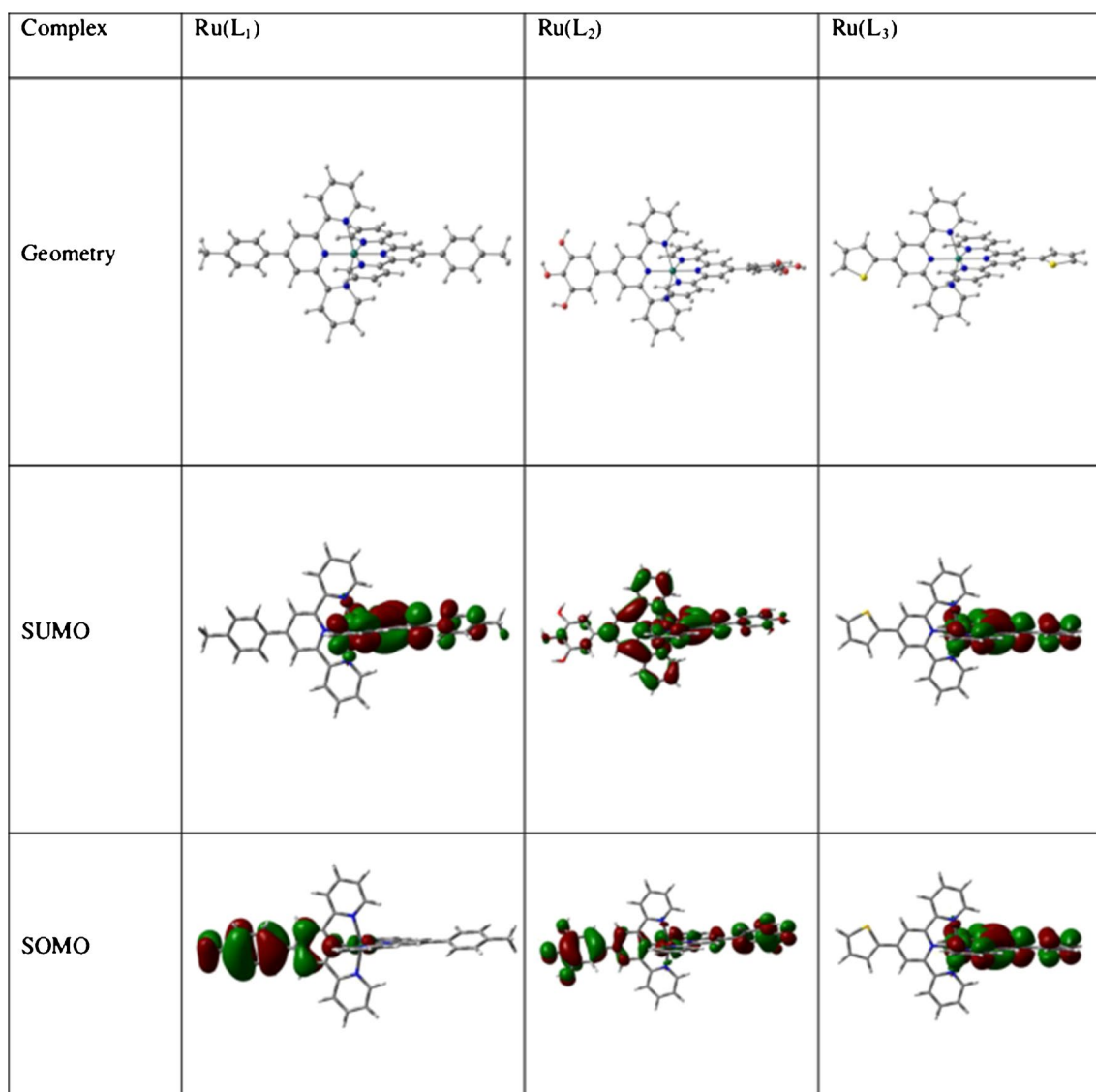


**Fig. 1** Optimized geometry and electronic distribution of the frontier orbitals for Ru(III) terpy complexes (RuL<sub>1</sub>-L<sub>3</sub>)

molecular orbitals of Ru(III) are more stable as they are located at lower energy levels.

## Results and Discussion

### UV-Vis Absorbance Spectra

The study of photophysical properties of Ru(III)-based terpy complex is of great interest to researchers because of their potential in optoelectronic applications. To investigate the influence of the electron-donating substituent on terpy of Ru(III) complex, its photophysical properties, such as UV-Vis absorption and PL spectra were evaluated. The UV-Vis absorption spectra of **Ru(L<sub>1</sub>-L<sub>3</sub>)** complexes

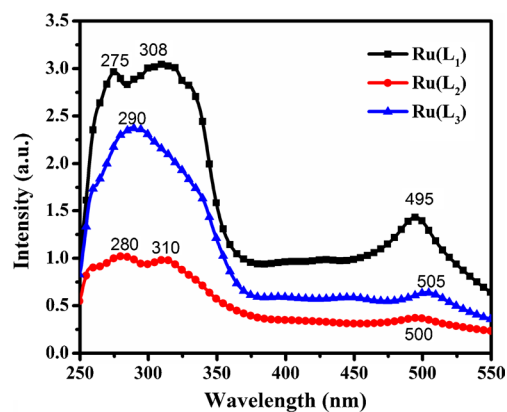


**Fig. 2** UV-Vis absorbance spectra of Ru(L<sub>1</sub>-L<sub>3</sub>) complexes in DMSO

in DMSO solution at room temperature are shown in Fig. 2. All complexes exhibit high intense absorption bands (250–350 nm) in UV region and less intense absorption bands in the visible region (495–505 nm).

The former are due to  $\pi-\pi^*$  and  $n-\pi^*$  of LC charge transition of terpyridine ligands and the latter to spin-allowed  $d-\pi^*$  of MLCT transition process [39]. The shorter wavelength bands of the spectra are attributed to transitions from SOMO/HOMO to higher energy orbitals. Two maximum absorption bands were observed for **Ru(L<sub>1</sub>)** and **Ru(L<sub>2</sub>)** complexes, while one was observed for **Ru(L<sub>3</sub>)** complex in the UV region of electromagnetic radiation. The maximum absorption peaks were observed at 275 and 308 nm for **Ru(L<sub>1</sub>)**, 280 and 310 nm for **Ru(L<sub>2</sub>)** and 290 nm for **Ru(L<sub>3</sub>)** complexes (Table 1). The bathochromic shifts of the maximum absorbance of 5 and 10 nm are seen for **Ru(L<sub>2</sub>)** and **Ru(L<sub>3</sub>)** complexes, respectively. The absence of second peak as expected around 310 nm in **Ru(L<sub>3</sub>)** complex could be due to the forbidden energy transition between Ru(III) and L<sub>3</sub> ligand. In the absorption spectra, some bands are centered at approximately 495, 500 and 505 nm for **Ru(L<sub>1</sub>)**, **Ru(L<sub>2</sub>)** and **Ru(L<sub>3</sub>)** complexes corresponding to the energy gap of 2.50, 2.48 and 2.46 eV, respectively, which are assigned to the electronic transition from SOMO to SUMO. The less intense and narrow absorption bands about 500 nm caused orange emission of these complexes. These bands could be due to d-d transition, which has been observed for similar ruthenium (IV) complexes [31, 40, 41]. These charge transition bands also depict the 5 and 10 nm bathochromic shift for **Ru(L<sub>2</sub>)** and **Ru(L<sub>3</sub>)** complexes, respectively. Hence, the electron-donating substituents of 3,4,5-trimethoxyphenyl and 4-thiophenyl group on terpy would have caused the red shift of **Ru(L<sub>2</sub>)** and **Ru(L<sub>3</sub>)** complexes compared to **Ru(L<sub>1</sub>)** complex. No significant bands were observed for the metal-centered (MC) charge transition of all Ru(III) complexes.

### Photoluminescence Spectra

The PL spectra were recorded on excitation at 310 nm for **Ru(L<sub>1</sub>)** and **Ru(L<sub>2</sub>)** complexes, while 290 nm for **Ru(L<sub>3</sub>)** complex corresponds to the maximum absorption wavelength of the complexes. The PL spectra of **Ru(L<sub>1-3</sub>)** complexes are shown in Fig. 3. A summary of photophysical data of three complexes is presented in Table 1. The PL spectra

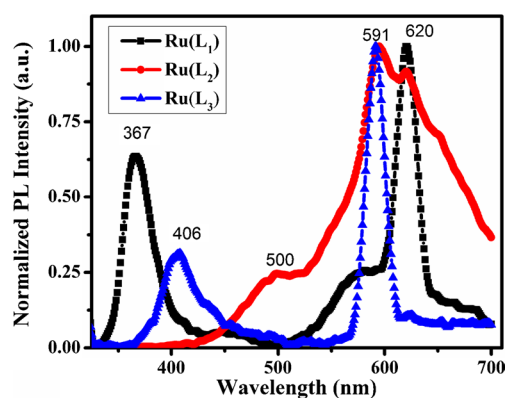


**Fig. 3** PL spectra of **Ru(L<sub>1-3</sub>)** complexes recorded at excitation wavelength of 310 nm for **Ru(L<sub>1</sub>)** and **Ru(L<sub>2</sub>)** complexes, whereas 290 nm for **Ru(L<sub>3</sub>)** complex in DMSO

show that the maximum emission bands are in the visible region of the electromagnetic spectrum. The dilute solution of Ru(III) complexes in DMSO shows a strong orange emission in the wavelength range starting from 591 to 620 nm. These emission bands could be due to the MLCT process of the complexes as confirmed by UV–Vis absorption spectra [42]. The absorption maximum of the spin-allowed MLCT band in the visible region for  $\text{Os}(\text{terpy})^{2+}$  lies at the same wavelength as that of  $\text{Ru}(\text{terpy})$  [41, 43].

Further, the emission maximum band in the visible region for **Ru(L<sub>2</sub>)** complex lies at the same wavelength as that of **Ru(L<sub>3</sub>)** complex, but the emission maximum was observed at 591 nm. This could be due to the more covalent characteristic nature of the MLCT transition in the Ru(III) complexes [44]. Since **Ru(L<sub>2</sub>)** and **Ru(L<sub>3</sub>)** complexes have the same emission maximum bands it is believed that the same MLCT contributed for these two complexes too. The maximum emission band was observed at 620 nm for **Ru(L<sub>1</sub>)** complex, and the shoulder peak was at 620 nm for **Ru(L<sub>2</sub>)** complex. All these transitions take place in the lower energy transition from MLCT to the ground state [45]. In addition, the **Ru(L<sub>2</sub>)** complex has the broadened emission spectrum compared to **Ru(L<sub>1</sub>)** and **Ru(L<sub>3</sub>)** complexes in the visible region. This broad emission of the **Ru(L<sub>2</sub>)** complex could be due to the more electron-donating nature of the 3,4,5-trimethoxyphenyl substituent (to terpy ligand on Ru(III)). The luminescence band of the **Ru(L<sub>2</sub>)** and **Ru(L<sub>3</sub>)** complexes

**Table 1** Synthetic route of Ru(III) terpyridine complexes (**RuL<sub>1-3</sub>**)

Complexes	Absorption ( $\lambda_{\text{max}}$ )		Emission ( $\lambda_{\text{max}}$ )	Optical band gap (eV)	Fluorescence Lifetime (ns)	Melting point ( $^{\circ}\text{C}$ )
	LC	MLCT				
<b>Ru(L<sub>1</sub>)</b>	275, 308	459	620	2.50	0.27	425
<b>Ru(L<sub>2</sub>)</b>	280, 310	500	591	2.48	0.46	429
<b>Ru(L<sub>3</sub>)</b>	290	505	591	2.46	0.52	471

was considerably shifted to the blue by 29 nm compared to **Ru(L<sub>1</sub>)** complex. Further, less-intense emission bands were observed at 367, 406 and 500 nm for **Ru(L<sub>1</sub>)**, **Ru(L<sub>2</sub>)** and **Ru(L<sub>3</sub>)** complexes, respectively, probably due to charge transition between LC transitions of terpy ligands. The red shifts are consistent with the LC charge transition of the UV–Vis absorption maximum. The bands centering at approximately 591 and 620 nm demonstrate that the emissions originated from the transition of SUMO to SOMO, that is, the radiative decay from the doublet excitons.

### Cyclic Voltammetry

The redox properties of the **Ru(L<sub>1</sub>-L<sub>3</sub>)** complexes were studied by measurement with CV in a three-electrode cell system. Tetrabutylammonium perchlorate (TBAP) (0.1 M) was dissolved in acetonitrile (ACN) and used as an electrolyte solution with ferrocene (Fc) as an internal standard. Figure 4 shows the cyclic voltammogram of the **Ru(L<sub>1</sub>)** complex in the potential range between  $-1.4$  and  $+2.0$  V at a scan rate of  $100 \text{ mV s}^{-1}$ . The electrochemical properties of the Ru(III) complexes are mainly dependent on the influence of Ru(III) ions and not of terpy ligands [46]. Hence, the **Ru(L<sub>1</sub>)** complex was considered to discuss the electrochemical properties of the Ru(III) complex. All three Ru(III) complexes show a similar redox behaviour. The three redox couples have been observed in the potential range of  $1.1$  to  $-0.4$  V for the **Ru(L<sub>1</sub>)** complex. The electrochemical data for the three Ru(III) complexes is listed in Table 1. Further, it has been noticed that the all complexes show a good reversible redox process.

The cathodic peak  $C_{\text{III} \rightarrow \text{II}}$  at a potential of  $0.35$  V and the anodic peak  $A_{\text{II} \rightarrow \text{III}}$  at a potential of  $0.55$  V correspond to the reduction of Ru(III) to Ru(II) and the oxidation of Ru(II) to Ru(III), respectively [47]. Moreover, the second redox

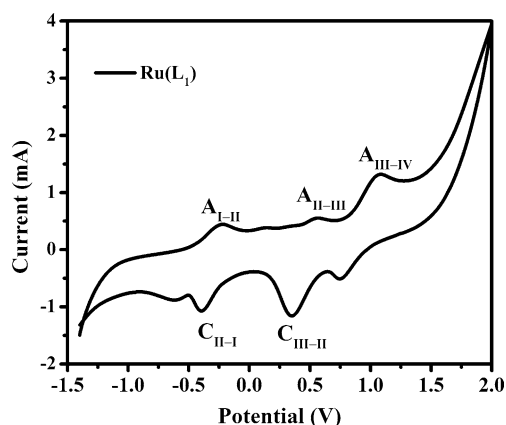


**Fig. 4** Cyclic voltammogram of **Ru(L<sub>1</sub>)** complex in acetonitrile (vs. SCE). The process at about  $0.25$  V is due to ferrocene, added as a reference

couple is associated with successive reduction of Ru(II) to Ru(I) (peaks  $C_{\text{II} \rightarrow \text{I}}$  at the potential of  $-0.40$ ) and correspond with the oxidation of Ru(I) to Ru(II) (peaks  $A_{\text{I} \rightarrow \text{II}}$  at the potential of  $-0.22$  V), respectively. The additional anodic peak at  $A_{\text{III} \rightarrow \text{IV}}$  observed at a potential of  $1.08$  V could be attributed to the oxidation of Ru(III) to Ru(IV). This peak is associated with a cathodic peak potential of  $0.75$  V, which can be due to the reduction of Ru(IV) to Ru(III) [48].

### Thermal Properties

The thermal properties of the three **Ru(L<sub>1</sub>-L<sub>3</sub>)** complexes are characterised by TGA and DSC analysis. The  $T_d$ ,  $T_g$  and  $T_m$  of these complexes were systematically studied. Figure 5 shows the DSC curves of the **Ru(L<sub>1</sub>-L<sub>3</sub>)** complexes under nitrogen atmosphere, while the samples were heated up from room temperature to slightly above their melting temperature at a scanning rate of  $10 \text{ }^\circ\text{C min}^{-1}$ .

It is observed that all the Ru(III) complexes have an endothermic peak, which shows the melting point of the complexes. The observed melting temperatures were  $425$ ,  $429$  and  $471$   $^\circ\text{C}$  for **Ru(L<sub>1</sub>)**, **Ru(L<sub>2</sub>)** and **Ru(L<sub>3</sub>)** complexes, respectively. The melting point of the **Ru(L<sub>1</sub>)** and **Ru(L<sub>3</sub>)** complexes shows sharp endothermic peaks, whereas it is a broad endothermic peak for the **Ru(L<sub>2</sub>)** complex. Among the three Ru(III) complexes, **Ru(L<sub>3</sub>)** has a higher  $T_m$  than the other two Ru(III) complexes, and hence, **Ru(L<sub>3</sub>)** complex is thermally more stable [49]. The DSC thermograms of Ru(III) complexes show no signature of  $T_g$  and crystalline

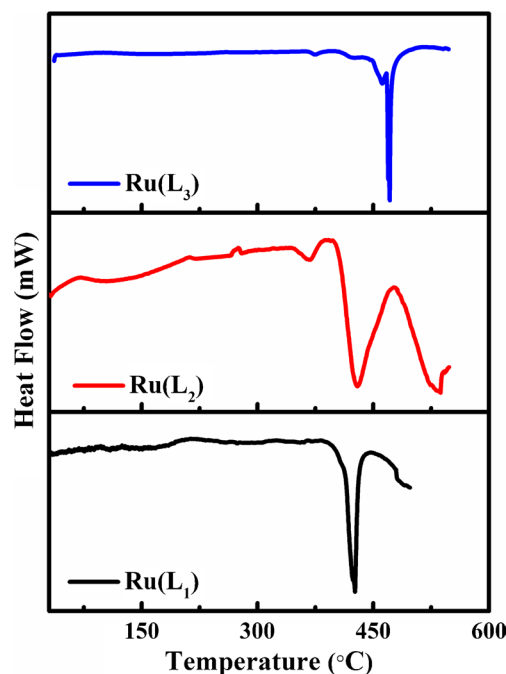


**Fig. 5** DSC plots of the **Ru(L<sub>1</sub>-L<sub>3</sub>)** complexes

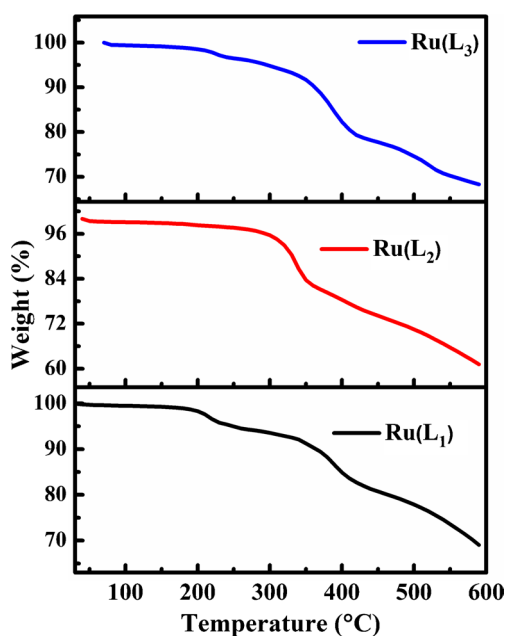


**Fig. 6** TGA thermogram of Ru(L1-L3) complexes

temperature ( $T_c$ ). However, the thermogram of the Ru(III) complexes shows a small inflection (exothermic peak) at a low temperature, which could be due to the elimination of volatile substrate. In conclusion, all the three complexes are thermally very stable as well as crystalline. The observed degradation temperatures are 202, 310 and 210 °C for **Ru(L<sub>1</sub>)**, **Ru(L<sub>2</sub>)** and **Ru(L<sub>3</sub>)** complexes, respectively (see Fig. 6). **Ru(L<sub>2</sub>)** complex shows higher degradation temperature and thermal stability than the other two Ru(III) complexes [50]. It is observed that no significant weight loss takes place at low temperatures. Hence, these complexes exhibit a good thermal stability with  $T_d$  (thermal-decomposition temperature at a wt.% of 95) in the range 250–313 °C. The observed weight losses of 5% were 250, 313 and 297 °C for the **Ru(L<sub>1</sub>)**, **Ru(L<sub>2</sub>)** and **Ru(L<sub>3</sub>)** complexes, respectively.

The maximum rate of weight loss  $T_d$  (thermal-decomposition temperature at a wt.% of 39%) takes place at 590 °C for **Ru(L<sub>2</sub>)** complex. Moreover, around 70 wt% of the residue composed of ruthenium ash and remained above 590 °C for the **Ru(L<sub>1</sub>)** and **Ru(L<sub>3</sub>)** complexes. Compared to the free ligand, the metal complexes revealed a significant increase in thermal stability, as can be seen from the temperature onset of a 5% weight loss [51]. Hence, Ru(III) complexes are more stable on exposure to air and showed high thermal stability in nitrogen atmosphere.

### Fluorescence Lifetime Measurements

The lifetime of luminescence is an important parameter as the luminescence property of a material depends on it.

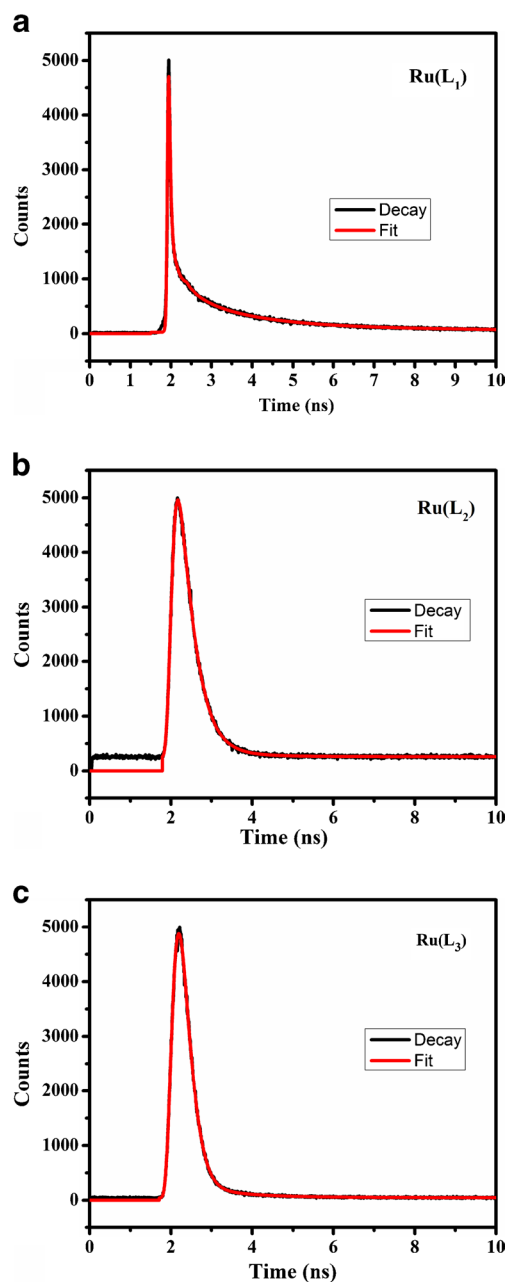


**Fig. 7** Fluorescence decay spectra of Ru(L<sub>1</sub>) **a**, Ru(L<sub>2</sub>) **b** and Ru(L<sub>3</sub>) **c** complexes at the excitation wavelength of 310 nm with one-exponential fit residuals,  $\chi^2 = 1.002$

Figure 7 shows the fitted decay curve of **Ru(L<sub>1</sub>-L<sub>3</sub>)** complexes in DMSO obtained by using the TCSPC method under laser excitation at 310 nm with a 96.8 ps pulse width. The luminescence decay spectra of the three complexes were fitted by a single exponential decay function. The observed lifetimes are 0.27, 0.46 and 0.52 ns for **Ru(L<sub>1</sub>)**, **Ru(L<sub>2</sub>)** and **Ru(L<sub>3</sub>)**, respectively. Hence, the measured lifetime of the **Ru(L<sub>3</sub>)** complex is significantly longer than the other two Ru(III) complexes.

It has been reported that the longer conjugation length in the ligand leads to longer lifetime [52]. The short-lived fluorescence of  $\text{Ru}(\text{L}_1)$  might be assigned to the strong intramolecular coupling interaction of trimethoxy fluorophores which lead to the fast charge transfer process. The lifetime on the nanosecond time scale indicates that the three Ru(III) complexes have the fluorescent character of the luminescence.

### Scanning Electron Microscope

The surface morphology of the synthesised  $\text{Ru}(\text{L}_1\text{-L}_3)$  complexes was analysed by SEM as depicted in Fig. 8. Figure 8a shows an SEM micrograph of the  $\text{Ru}(\text{L}_1)$  complex, where cauliflower-like structural particles have been observed. The size of the particles ranges from 5 to 10  $\mu\text{m}$  and the inset shows a clear cauliflower-like structural particle of  $\text{Ru}(\text{L}_1)$ . Figure 8b depicts the cauliflower-like structure along with one-dimensional nano rod of the  $\text{Ru}(\text{L}_2)$  complex with the diameter ranging from 7 to 12  $\mu\text{m}$  and the length being about a few micrometers. Moreover, the SEM image of the  $\text{Ru}(\text{L}_3)$  complex, as shown in Fig. 8c shows one-dimensional micro-rod structures with diameters of around 3  $\mu\text{m}$  and about 7  $\mu\text{m}$  length. The SEM images of the complexes reveal that the  $\text{Ru}(\text{L}_2)$  complex has more surface area and a greater surface-to-volume ratio which could enhance the luminescence properties [53].

### Conclusion

In conclusion, three novel Ru(III) complexes were synthesised and their photophysical, electrochemical and thermal properties were studied by varying the electron-donating substituents at the 4'-position of the 2,2':6',2''-terpyridine ring. Spectral analysis showed that electroluminescence of the OLED originated from electron transition between SUMO and SOMO. These complexes exhibit high thermal stability without any significant weight loss below 250  $^{\circ}\text{C}$ . All the complexes show good PL emissions in a DMSO solution with a broad emission spectrum ca. 591–620 nm. The  $\text{Ru}(\text{L}_2)$  complex exhibits a broad orange emission compared to  $\text{Ru}(\text{L}_1)$  and  $\text{Ru}(\text{L}_3)$  complexes. The measurements of the excited state lifetime confirm that the potential charge transfer to the  $\pi\text{-}\pi^*$  state of the MLCT state in the complexes is efficient. The bands centered on 591 and 620 nm demonstrate that these emissions originated from the transition of SUMO to SOMO, that is, from radiative decay from the doublet exciton. These observations imply that by simply changing the terminal the substituent can lead to various optical properties, such as deep orange emission for the three  $\text{Ru}(\text{L}_1\text{-L}_3)$  complex. Although the devices using these complexes have not been demonstrated in this work and are beyond the scope of the

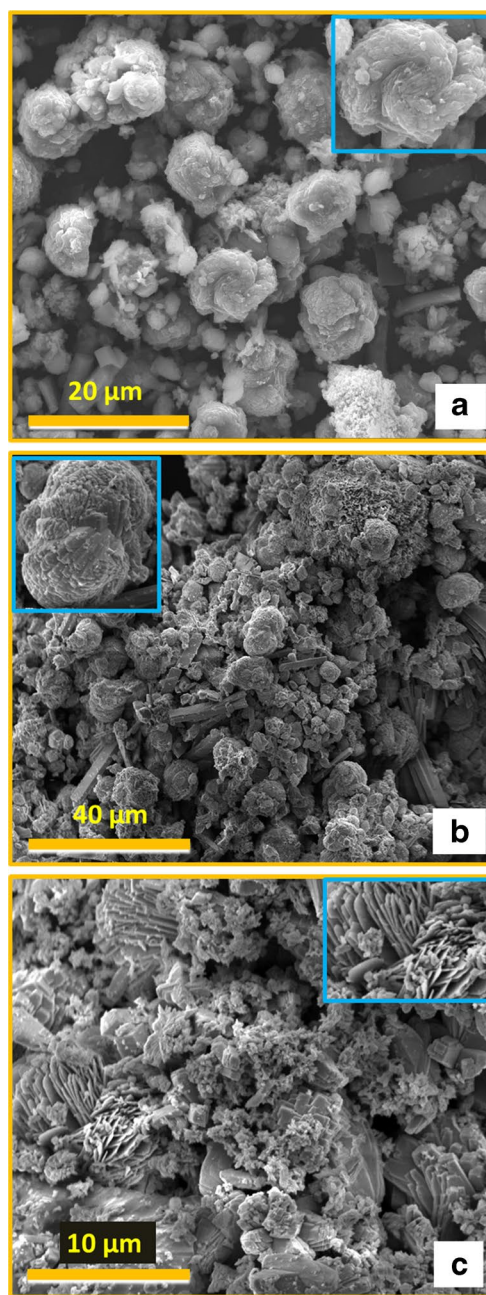


**Fig. 8** SEM images of **a**  $\text{Ru}(\text{L}_1)$ , **b**  $\text{Ru}(\text{L}_2)$  and **c**  $\text{Ru}(\text{L}_3)$  complexes

current discussion, it is believed that the OLEDs based on them would exhibit a promising performance according to the current results and have potential electron-transporting properties from terpyridine derivatives.

**Acknowledgements** We thank the Council of Scientific and Industrial Research (CSIR), Government of India for financial support. The authors would like to acknowledge the Supercomputer Education and Research Centre (SERC), Indian Institute of Science, Bangalore, India for providing the computational facility.

## References

- Jou JH, Su YT, Hsiao MT, Yu HH, He ZK, Fu SC, Chiang CH, Chen CT, Chou CH, Shyue JJ (2016) Solution-process-feasible Deep-red phosphorescent emitter. *J Phys Chem C* 120:18794–11802
- Nagai Y, Sasabe H, Takahashi J, Onuma N, Ito T, Ohisa S, Kido J (2017) Highly efficient, deep-red organic light-emitting devices using energy transfer from exciplexes. *J Mater Chem C* 5:527–530
- Sun Y, Stephen RF (2008) Enhanced light out-coupling of organic light-emitting devices using embedded low-index grids. *Nat Photon* 2:483–487
- Wood CD, Jone CW, Claverly JD, Blakesley JC, Giusca C, Castro FA (2017) Transient photocurrent and photo voltage mapping for characterisation of defects in organic photovoltaics. *Sol Energ Mat Sol Cells* 161:89–95
- Jayabharathi J, Ramanathan P, Karunakaran C, Thanikachalam V (2016) Fused methoxynaphthyl phenanthrimidazole semiconductors as functional layer in high efficient OLEDs. *J Fluoresc* 26:307–316
- Kim KH, Liao JL, Lee SW, Sim B, Moon C-K, Lee G-H, Kim HJ, Chi Y, Kim J-J (2016) Crystal organic light-emitting diodes with perfectly oriented non-doped Pt-based emitting layer. *Adv Mater* 28:2526–2532
- Constable EC, Alexander MWCT, Armaroli N, Balzani V, Maestri M (1992) Ligand substitution patterns control photophysical properties of ruthenium(ii)-2,2':6',2''-terpyridine complexes-room temperature emission from [ru(tpy)]<sub>2</sub> + analogues. *Polyhedron* 11:2707–2709
- Seino Y, Inomata S, Sasabe H, Pu YJ, Kido (2016) High-performance green OLEDs using thermally activated delayed fluorescence with a power efficiency of over 100 lm W<sup>-1</sup>. *J Adv Mater* 28:2638–2643
- Wang D, Xu QL, Zhang S, Li HY, Wang CC, Li TY, Jing YM, Huang W, Zheng YX, Accorsi G (2013) Synthesis and photoluminescence properties of rhenium(I) complexes based on 2,2':6',2''-terpyridine derivatives with hole-transporting units. *Dalton Trans* 42:2716–2723
- Juris A, Balzani V, Barigelletti F, Campagna S, Belser P, Zelewsky AV (1988) Ru(II) polypyridine complexes: photophysics, photochemistry, electrochemistry, and chemiluminescence. *Coord Chem Rev* 84:85–277
- Barthelmes K, Kubel J, Winter A, Wachtler M, Friebe C, Dietzek B, Schubert US (2015) New ruthenium bis(terpyridine) methanofullerene and pyrrolidinofullerene complexes: synthesis and electrochemical. *Photophysical Properties Inorg Chem* 54:3159–3171
- Medlycott EA, Hanan GS (2005) Designing tridentate ligands for ruthenium(II) complexes with prolonged room temperature luminescence lifetimes. *Chem Soc Rev* 34:133–142
- Medlycott EA, Hanan GS (2006) Synthesis and properties of mono- and oligo-nuclear Ru (II) complexes of tridentate ligands: the quest for long-lived room temperature excited states. *Coord Chem Rev* 250:1763–1782
- Jiang H, Lee SJ, Lin W (2002) Chiral hybrid metal – organic dendrimers. *Org Lett* 4:2149–2152
- Chaignon F, Torroba J, Blart E, Borgstrom M, Hammarstrom L, Odobel F (2005) Distance-independent photoinduced energy transfer over 1.1 to 2.3 nm in ruthenium trisbipyridine–fullerene assemblies. *New J Chem* 29:1272–1284
- Allen BD, Benniston AC, Harriman A, Mallon LJ, Pariani C (2006) Competing through-space and through-bond, intramolecular triplet-energy transfer in a supposedly rigid ruthenium(II) tris(2,2'-bipyridine)–fullerene molecular dyad. *Phys Chem Chem Phys* 8:4112–4118
- Kelch S, Rehahn M (1999) Rod-like ruthenium(II) coordination polymers: synthesis and properties in solution. *Chem Commun* 0:1123–1124
- Wild A, Winter A, Schlutter F, Schubert US (2011) Advances in the field of  $\pi$ -conjugated 2,2':6',2''-terpyridines. *Chem Soc Rev* 40:1459–1511
- Rudmann H, Shimada S, Rubner MF (2002) Solid-state light-emitting devices based on the tris-chelated ruthenium(II) complex. 4. high-efficiency light-emitting devices based on derivatives of the tris (2,2'-bipyridyl) ruthenium(II) complex. *J Am Chem Soc* 124:4918–4921
- Chmielewski PJ, Latos-Grazynski L, Pacholska E (1994) Low-valent nickel thiaporphyrins nuclear magnetic resonance and electron paramagnetic resonance studies. *Inorg Chem* 33:1992–1999
- Latos-Grazynski L, Lisowski J, Olmstead MM, Balch AL (1989) Five-coordinate complexes of 21-thiaporphyrin. Preparations, spectra, and structures of iron (II), nickel (II), and copper (II) complexes. *Inorg Chem* 28:3328–3331
- Umamahesh B, Karthikeyan NS, Sathiyarayanan KI, Malicka JM, Cocchi M (2016) Tetrazole iridium(III) complexes as a class of phosphorescent emitters for high-efficiency OLEDs. *J Mater Chem C* 4:10053–10060
- Kusamoto T, Kume S, Nishihara H (2008) Realization of SOMO – HOMO level conversion for a TEMPO-Dithiolate ligand by coordination to platinum(II). *J Am Chem Soc* 130:13844–13845
- Reineke S, Lindner F, Schwartz G, Schwartz G, Seidler N, Walzer K, Lussem B, Leo K (2009) White organic light-emitting diodes with fluorescent tube efficiency. *Nature* 459:234–238
- De Silva AP, Gunaratne HQN, Gunnlaugsson T, Huxley AJM, McCoy CP, Rademacher J, Rice TE (1997) Signaling recognition events with fluorescent sensors and switches. *Chem Rev* 97:1515–1565
- Vogtle F (1993) *Supramolecular Chemistry*. Wiley, Chichester
- Kosaka W, Itoh M, Miyasaka H (2015) The effect of chlorine and fluorine substitutions on tuning the ionization potential of benzoate-bridged paddlewheel diruthenium(II, II) complexes. *Dalton Trans* 44:8156–8168
- Mishra D, Naskar S, Butcher RJ, Chattopadhyay SK (2005) Ruthenium(II/III) mediated transformation of 1,2-bis(2'-pyridyl)methyleneimino benzene (L) to 2-(2'-benzimidazolyl)pyridine (L/H) and its in situ formed complexes with Ru(II) : X-ray structure of *trans*-[Ru(PPh<sub>3</sub>)<sub>2</sub>(L/H)<sub>2</sub>](ClO<sub>4</sub>). *Inorg Chim Acta* 358:3115–3121
- Motokawa N, Matsunaga S, Takaishi S, Miyasaka H, Yamashita M, Dunbar KR (2010) Reversible magnetism between an antiferromagnet and a ferromagnet related to solvation/desolvation in a robust layered [Ru<sub>2</sub>]TCNQ charge-transfer system. *J Am Chem Soc* 132:11943–11951
- Vögtle F, Plevoets M, Nieger M, Azzellini GA, Credi A, Cola LD, Marchis VD, Venturi M, Balzani V (1999) Dendrimers with a photoactive and redox-active [Ru(bpy)<sub>3</sub>]<sup>2+</sup>-type core: photophysical properties, electrochemical behavior, and excited-state electron-transfer reactions. *J Am Chem Soc* 121:6290–6298
- Jablonska-Wawrzycka A, Rogala P, Michałkiewicz S, Hodorowicz B, Barszcza B (2013) Ruthenium complexes in different oxidation states: synthesis, crystal structure, spectra and redox properties. *Dalton Trans* 42:6092–6101
- Clarke MJ (2003) Ruthenium metallopharmaceuticals. *Coord Chem Rev* 236:209–233
- Van der Drift RC, Bouwman E, Drent E (2002) Homogeneously catalysed isomerisation of allylic alcohols to carbonyl compounds. *J Organomet Chem* 650:1–24
- Tianzhi Yu Chengcheng, Zhang Yuling, Zhao ShaoQiang, Guo Peng, Liu Wentao, Li, Duowang Fan (2013) Synthesis, crystal structure and photoluminescence of a cyclometalated Iridium(III) coumarin complex. *J Fluoresc* 23:777–783

35. Lakshmanan R, Shivaprakash NC, Sindhu S (2015) Spectral characterizations and photophysical properties of one-step synthesized blue fluorescent 4'-aryl substituted 2, 2': 6', 2''-terpyridine for OLEDs application. *J Lumin* 168:145–150
36. Frisch MJ et al (2009) Gaussian 09, revision A.02. Gaussian, Inc., Wallingford, CT
37. Miyasaka H, Campos-Fernández CS, Clérac R, Dunbar KR (2000) Hexagonal layered materials composed of  $[M_2(O_2CCF_3)_4]$  ( $M = Ru$  and  $Rh$ ) donors and TCNQ acceptors. *Angew Chem Int Ed* 39:3831–3835
38. Motokawa N, Oyama T, Matsunaga S, Miyasaka H, Sugimoto K, Yamashita M, Lopez N, Dunbar KR (2008) A ladder based on paddlewheel diruthenium(II, II) rails connected by TCNQ rungs: a polymorph of the hexagonal 2-D network phase. *Dalton Trans* 4099–4102
39. Stone ML, Crosby GA (1981) Charge-transfer luminescence from ruthenium(II) complexes containing tridentate ligands. *Chem Phys Lett* 79:169–173
40. Coe BJ, Thompson DW, Culbertson CT, Schoonover JR, Meyer TJ (1995) Synthesis and photophysical properties of mono(2,2',2''-terpyridine) complexes of ruthenium(II). *Inorg Chem* 34:3385–3395
41. Constable EC, Housecroft CE, Schofield ER, Encinas S, Armaroli N, Barigelletti F, Flamigni L, Figgemeier L, Vos JG (1999) Luminescent molecular wires with 2,5-thiophenediyl spacers linking  $\{Ru(terpy)_2\}$  units. *Chem Commun* 869–870
42. Priyarega S, Muthu tamizh M, Karvembu R, Prabhakaran R, Natarajan K, (2011) Synthesis, spectroscopic characterization and catalytic oxidation properties of ONO/ONS donor schiff base ruthenium(III) complexes containing PPh<sub>3</sub>/AsPh<sub>3</sub>. 123:313–325
43. Winkler JR, Netzel TL, Creutz C, Sutin N (1987) Direct observation of metal-to-ligand charge-transfer (MLCT) excited states of pentaammineruthenium(II) complexes. *J Am Chem Soc* 109:2381–2392
44. Hutchison K, Morris JC, Nile TA, Walsh JL (1999) Spectroscopic and photophysical properties of complexes of 4'-ferrocenyl-2,2':6',2''-terpyridine and related ligands. *Inorg Chem* 38:2516–2523
45. Sinkeldam RW, Greco NJ, Tor Y (2010) Fluorescent analogs of biomolecular building blocks: design, properties, and applications. *Chem Rev* 110:2579–2619
46. Santoni MP, Medlycott EA, Hanan GS, Hasenknopf B, Proust A, Nastasi F, Campagna S, Chiorboli C, Argazzid R, Scandola F (2009) Photoinduced energy transfer in a rod-like dinuclear Ru(II) complex containing bis-pyridyl-1,3,5-triazine ligands.. *Dalton Trans* 3964–3970
47. Breivogel A, Hempel K, Heinze K (2011) Inorg. Dinuclear bis (terpyridine) ruthenium (II) complexes by amide coupling of ruthenium amino acids: synthesis and properties. *Chim Acta* 374:152–162
48. Brown DG, Sanguantrakun N, Schulze B, Schubert US, Berlinguette CP (2012) Bis(tridentate) ruthenium-terpyridine complexes featuring microsecond excited-state. *Lifetimes J Am Chem Soc* 134:12354 – 12357
49. Amirnasr M, Nazeeruddin MK, Gratzel M (2000) Thermal stability of cis-dithiocyanato(2,2'-bipyridyl-4,4'-dicarboxylate) ruthenium(II) photosensitizer in the free form and on nanocrystalline TiO<sub>2</sub> films. *Thermochim Acta* 348:105–114
50. Gherab KN, Gatri R, Hank Z, Dick B, Kutta RJ, Winter R, Luc J, Sahraoui B, Fillaut JL (2010) Design and photoinduced surface relief grating formation of photoresponsive azobenzene based molecular materials with ruthenium acetylides. *J Mater Chem* 20:2858–2864
51. Nazeeruddin MK, Amirnasr M, Comte P, Mackay JR, McQuillan AJ, Houriet R, Gratzel M (2000) Adsorption studies of counterions carried by the sensitizer cis-dithiocyanato(2,2'-bipyridyl-4,4'-dicarboxylate) ruthenium(II) on nanocrystalline TiO<sub>2</sub> Films. *Langmuir* 16:8525–8528
52. McCusker CE, Chakraborty A, Castellano FN (2014) Excited state equilibrium induced lifetime extension in a dinuclear platinum(II) complex. *J Phys Chem A* 118:10391 – 10399
53. Hu JS, Ji HX, Cao AM, Huang ZX, Zhang Y, Wan LJ, Xia AD, Yu DP, Meng XM, Lee ST (2007) Facile solution synthesis of hexagonal Alq<sub>3</sub> nanorods and their field emission properties. *Chem Commun* 3083–3085